Continuous high-purity bioelectrochemical nitrogen recovery from high N-loaded wastewaters

Zainab Ul [4], Mira Sulonen [3], Juan Antonio Baeza [1,*], Albert Guisasola [2]

GENOCOV, Departament d'Enginyeria Química, Biològica i Ambiental, Escola d'Enginyeria, Universitat Autònoma de Barcelona, 08193 Bellaterra (Cerdanyola del Vallès), Barcelona, Spain

ARTICLE INFO

ABSTRACT

Microbial electrolysis cells (MEC) have been identified as an energy efficient system for ammonium recovery from wastewater. However, high ammonium concentrations at the anode can have inhibitory effects. This work aims to determine the effects on current generation performance and active ammonia nitrogen recovery in wastewater containing 0.5 to 2.5 g $N-NH_4^+$/L. The study also evaluates the effect of two cathode materials, stainless steel (SS-MEC) and nickel foam (NF-MEC). When the concentration of ammonium in the feed was increased from 0.5 to 1.5 g $N-NH_4^+$/L the maximum current density increased from 3.2 to 3.9 A/m^2, but a further increase to 2.5 g $N-NH_4^+$/L inhibited the biofilm activity, decreasing the current density to 0.5 A/m^2. The maximum ammonium removal and recovery efficiencies were 71 % and 33 % at 0.5 g $N-NH_4^+$/L. The SS-MEC exhibited more energy efficient ammonium recovery compared to the NF-MEC, requiring 3.6 kWh/kg$_{N,recovered}$ at 0.5 gN-NH4+/L. The highest ammonium recovery rate of 33 g$_N$/m^2/d (1.5 gN-NH$_4^+$/L) was obtained with an energy consumption of 4.5 kWh/kg$_{N,recovered}$. Conversely, a lower recovery rate (10 g$_N$/m2/d for 2.5 gN-NH$_4^+$/L) resulted in reduced energy consumption at 2.1 kWh/kg$_{N,recovered}$. This highlights the inherent trade-off between energy consumption and efficient ammonium recovery in the process.

1. Introduction

The removal of ammonium from wastewater is essential due to its contribution to water body eutrophication [1]. Several methods, including biological and physicochemical techniques such as nitrification, denitrification, ion exchange, air stripping, and membrane processes, have been employed to remove ammonium from wastewater [2–5]. Since ammonium is a crucial fertilizer component used in agriculture, transitioning from mere removal to recovery is vital for establishing a sustainable future [6]. Embracing a circular economy approach, bioelectrochemical systems (BES) stands out as a promising solution for directly recovering ammonium from wastewater and transforming it into fertilizer [7]. Over the last few years, ammonium recovery from wastewater by BES has been scrutinized as an alternative to converting ammonium to nitrogen via nitrite or nitrate [8].

The recovery of ammonium in BES hinges on the electrical current

[9]. This current facilitates the movement of electrons, serving as the driving force to transport positively charged ammonium ions through a cation exchange membrane (CEM) [10,11]. Within BES, electrons are generated at the anode through the oxidation of organic matter by anode-respiring bacteria (ARB) into electrons, protons, and carbon dioxide. Depending on the reduction reaction taking place at the cathode, the energy can either be harvested as electricity in the so called microbial fuel cells or necessitate electrical energy input to drive the reactions in devices known as microbial electrolysis cells (MECs) [12,13].

Numerous factors, including nutrients, temperature, pH, toxic compounds, operational conditions, reactor design, and inoculum, can influence the performance of a BES. Ammonium transfer in particular depends significantly on the concentration gradient over the CEM. Thus, for profitable ammonium recovery, it is essential to treat high nitrogen loaded streams such as urine or reject water. However, such high concentrations of total ammonia nitrogen (TAN) can be a challenge due to

its toxicity [14–16]. TAN comprises two reactive nitrogen forms: ammonium and ammonia. The balance between these forms is determined by the pKa of the ammonia/ammonium equilibrium, which is 9.25 (at 25°C) [7]. The toxicity issue primarily lies with ammonia, a factor that intensifies with higher pH and temperature levels [15]. Ammonia has been identified as the active component causing inhibition in anaerobic biological processes [14,17–19]. Mechanisms such as disruption of enzymatic activity, disturbance of intracellular pH balance, and dehydration due to osmotic stress are widely acknowledged as the inhibitory effects of ammonia [20,21].

Nevertheless, the inhibitory impact of TAN in BES remains unresolved. There is ongoing debate regarding the concentration threshold at which TAN becomes toxic or inhibitory for ARB. This threshold value varies based on the specific microorganisms, operational conditions, pH, conductivity, and acclimation phase employed. Elevated TAN concentrations in the influent could potentially impair the activity of ARB and might hinder current generation and the treatment of organic contaminants [7]. The minimal reported TAN concentration that inhibits electricity generation is 0.5 g/L in a single-chambered MFC operated in batch mode [19]. In certain studies, inhibitory effects were noted at TAN concentrations of 2.2 and 2.5 g/L [22,23].

However, other studies [23,24] found no inhibition at TAN concentrations of 3.5 g/L and 3 g/L, respectively. Further research showed that ARB exhibited tolerance to TAN concentrations up to 4 g/L in MFCs, with no adverse effects [23,25–28]. Kuntke et al. [25] suggested that their lack of inhibition (testing TAN concentrations up to 4 g/L) might be due, in part, to the anolyte pH being lower than 7.1, resulting in lower ammonia concentrations. Interestingly, Wang et al. [28] observed no inhibitory effects on current generation at a TAN concentration of 4 g/L, despite the anodic effluent having a pH of 8. Some researchers hypothesize that the increase in current generation with higher TAN concentrations is due to enhanced conductivity [27]. Likewise, there was no detrimental impact on the performance of a MEC observed at a concentration of 5 g/L of TAN [29]. However, the performance decreased when the concentration was raised to 5.5 g/L. In a different study, no inhibitory effects were reported, even at TAN concentrations as high as 5.9 g/L, with an anolyte pH ranging from 7 to 7.5 [30].

Most of the adverse impacts of TAN concentration on current generation have been observed in MFCs operating in batch mode. The lack of consistency across different studies regarding the TAN concentration threshold is likely due to factors such as pH, oxygen diffusion from the cathode (nitrification) to the anolyte and the use of a CEM that enables the transfer of ammonium ions from the anode to the cathode chamber. These elements can lead to TAN loss from the anolyte, potentially reducing TAN inhibition [22].

Another crucial challenge when operating BES-driven ammonium recovery is generating sufficient electrical current to facilitate the movement of ammonium ions from the anolyte to the catholyte. In theory, for every electron serving as an electrical current, a positively charged cation should be transferred from the anolyte to the catholyte through the CEM [31]. Hence, researchers have introduced the concept of the load ratio (L_n) in the literature. This ratio is used to assess the charge balance between electrons as current and the ammonium loading [32]. A L_n value greater than 1 indicates an excess of current over ammonium, while a L_n value below 1 suggests an excess of ammonium over current. A L_n of 1 signifies that the current is adequate to transport all the ammonium from the anodic compartment to the cathodic compartment, assuming ammonium is the sole cation being transported across the membrane. Therefore, understanding L_n is crucial for determining the optimal operational threshold for the system.

Once ammonium ions are transferred into the cathode chamber, they transform into ammonia molecules due to the increased pH in the catholyte caused by the formation of hydroxide ions on the cathode surface [26,33]. These ammonia molecules can then be recovered from the catholyte, either through stripping [34] or by employing hydrophobic membranes [35]. In both scenarios, the ammonia can

subsequently be absorbed in an acidic solution [6,36]. However, air stripping is often impractical due to the need for aeration, substantial energy input, and the generation of a large volume of low-value off-gas [8]. Stripping as the recovery method has been reported to consume between 17-26 kWh per kg of removed ammonium [37,38]. Conversely, the hydrophobic membrane recovery method, based on ammonia gas permeation through the membrane pores and subsequent reaction with an acidic solution on the other side, has a lower energy demand and enable a simpler ammonia recovery process compared to stripping methods [36].

Since the migration of ammonium from the anolyte to the catholyte is dependent on the generated current, achieving higher current is desirable to prevent toxicity issues. Increased current facilitates the removal of ammonium ions from the anolyte, resulting in lower free ammonia concentration. In this context, the choice of cathode materials assumes a critical role, as different materials exhibit diverse catalytic properties and electrochemical behaviours. Therefore, the cathode material can impact the current generation and the efficiency of hydrogen production which is essential for elevating the pH of the catholyte. The pH increase is vital for converting ammonium ions into ammonia, which can subsequently be transported to the recovery chamber through a hydrophobic membrane. The interplay of these factors is complex, underscoring the importance of studying them to assess the performance of ammonium fed MECs.

Direct recovery of ammonium from municipal wastewater is often not economically viable due to the low nitrogen concentrations (<100 mg/L) commonly found [39]. However, in wastewater treatment plants (WWTPs), part of the nitrogen is used for microbial growth in the activated sludge process and then released back into the aqueous phase during the anaerobic digestion of the waste sludge [40]. Upon removing water from the digested sludge, the most concentrated nitrogen stream in the plant, known as reject water, is generated (with concentrations reaching up to 1-1.5 g/L) [41]. This reject water is usually recirculated back into the influent, imposing an unnecessary increase in the nitrogen load on WWTPs [39]. Therefore, the reject water can be considered a valuable stream for exploring ammonium recovery.
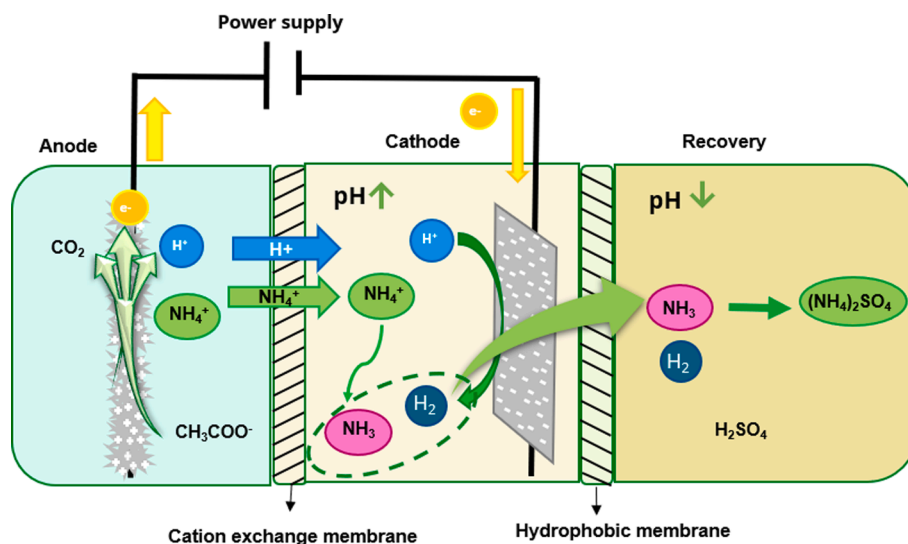
Considering the background described in this introduction, hydrophobic membranes have not been extensively studied as a method for ammonia recovery compared to the conventional stripping approach in MECs. Additionally, it is essential to confirm the adaptability of ARB to high ammonium concentrations before contemplating the practical implementation of a continuously fed MEC system treating reject water. Therefore, this study examines for the first time the inhibitory effects of ammonium on current generation and ammonium recovery in a continuously operated MEC with hydrophobic membrane and using synthetic reject water. The study also compares two different cathode materials: stainless steel mesh and nickel foam.

2. Materials and methods

2.1. BES design

Novel tailor-made bioelectrochemical reactors were designed to recover ammonium as ammonium sulphate using three chamber MECs. Each of the two flat plate MECs (total volume 0.8 L) used had one anode chamber (0.4 L), one cathode chamber (0.2 L) and one recovery chamber (0.2 L). The cathode chamber was separated from the anode chamber by a CEM (CMI-7000, Membrane International, NJ) and the recovery chamber was separated from the cathode chamber by a hydrophobic membrane (Tyvek (DuPont, US) with an area of 100 cm^2) (Schematic 1).

Two carbon brushes (75 mm length x 50 mm diameter, fibre diameter of 7.2 μm, Millrose Co., USA) served as the anode in the setup. Two different types of cathodes were tested: nickel foam (NF-MEC) (with a purity >99.99%, dimensions of 600/500 mm width, and porosity ≥ 95%; Recemat Ni4753.016) and stainless steel (SS-MEC) mesh (304,

Schematic 1. Conceptual diagram illustrating ammonia recovery in a three chamber MEC with an integrated recovery chamber.

Feval filtros, Spain). Titanium wire was employed as the current collector.

The anolyte was continuously circulated through the anode chamber at a rate of 0.5 mL/min via a peristaltic pump. Each condition (different ammonium concentration in the anolyte) was tested for two consecutive cycles, each cycle ending when the catholyte and recovery solutions were replaced after the ammonium concentration of the catholyte had remained stable for two consecutive days.

A fixed voltage of 1.4V was applied to whole cell by a power source (Programmable DC LAB Power supply LABPS3005DN, Velleman Group, Belgium). The current intensity was digitally logged every 5 minutes by measuring the voltage over an external resistor (10 Ω) using a 16-bit data acquisition card (Advantech PCI-1716) controlled with AddControl software, developed by the research group in LabWindows CVI.

2.2. Media and chemical analysis

The anolyte was a synthetic reject water that contained 104 mg/L Na_2HPO_4, 52 mg/L C_2H_5COONa, 103 NH_4HCO_3, 274 mg/L $KHCO_3$, 152 mg/L $CaCO_3$, 231 mg/L $MgCl_2·6H_2O$ and 1mL/L trace elements (1 g EDTA, 0.164 g $CoCl_2·6H_2O$, 0.228 g $CaCl_2·2H_2O$, 0.02 g H_3BO_3, 0.04 g $Na_2MoO_4·2H_2O$, 0.002 g Na_2SeO_3, 0.02 g $Na_2WO_4·2H_2O$, 0.04 g $NiCl_2·6H_2O$, 2.32 g $MgCl_2$, 1.18 g $MnCl_2·4H_2O$, 0.1 g $ZnCl_2$, 0.02 g $CuSO_4·5H_2O$ and 0.02 g $AlK(SO_4)_2$). The reject water was amended with NH_4HCO_3 to obtain the targeted inlet TAN concentrations ranging from 0.5 to 2.5 g $N-NH_4^+/L$, along with acetate to reach a COD concentration of 700 mg COD/L. The concentrations were tested in ascending order. The catholyte solution contained 4 g/L of sodium chloride, and the recovery solution was composed of 1% sulfuric acid. The anolyte and catholyte pH were measured using a pH probe (HACH pH electrode, Crison5233, Spain) and conductivity was measured using a conductivity meter (COND 8, XS Instruments, Italy). The characteristics of the anodic feed (ammonium concentration, pH, conductivity and calculated free

ammonia concentrations) are presented in Table 1.

The anode was inoculated with anaerobic sludge collected from a WWTP. Prior to starting experiments with different ammonium concentrations, the MECs were operated in batch mode for 23 days without additional ammonium until two satisfactory cycles were achieved, after which the experiments were initiated. Unlike the anolyte, the catholyte and recovery solution were not recirculated. Throughout the experiments, samples were collected daily from the anolyte, catholyte, and recovery solution.

The acetate concentration was analysed in the anolyte influent and effluent using a gas chromatograph (Agilent Technologies 7820-A) with a DB-FFAB column, following a method described elsewhere [42]. Sodium, potassium, and ammonium concentrations were determined using a Dionex DX120 ion chromatograph with AS40 autosampler, IonPac CS12A cation exchange column, CSRS 300 suppressor (4mm) (Thermo Fisher Scientific, USA), and 20 mM methanesulfonic acid as the eluent at a flow rate of 1 mL/min. Before analysing acetate and cation concentrations, samples were filtered using 0.22 μm filters (PTFE syringe filters, VWR, Amsterdam, The Netherlands).

2.3. Electrochemical techniques

Cyclic voltammetry (CV) were conducted on the MECs using a potentiostat (Nanoelectra NEV4, Spain) to characterize the anodic biofilm. A voltage ramp ranging from 0 V to 1 V, with a scan rate of 0.005 V s^{-1}, was applied to the working electrode. This process included a gradual increase in potential, followed by the reversal of the scan back to the initial potential. All electrochemical assays were carried out in the experimental media. The anode was employed as the working electrode, while the cathode served as a counter electrode and an Ag/AgCl electrode (3 mol L^{-1} KCl RE-1B, +210 vs. SHE, BAS Inc, Tokyo, Japan) was used as the reference electrode.

2.4. Calculations

The current density was standardized based on the projected surface area of the anode. The load ratio, defined as the ratio of current to ammonium loading, is represented by Eq. (1):

$$L_N = \frac{J_{applied}}{C_{NH4\_N,feed} \cdot Q_{feed} \cdot \frac{F}{A}} \tag{1}$$

Where $J_{applied}$ is the applied current density (A/m^2), $C_{NH4\_N, feed}$ is the NH_4^+ concentration in the feed (mol/m^3), Q_{feed} is the feed rate (m^3/s), F

Table 1
Conductivity, pH, and calculated free ammonia values in the anolyte for different inlet ammonium concentrations.

$[NH_4]_i$ (mgN/L)	Conductivity (mS/cm)	pH	$[NH_3]_i$ (mgN/L)
500	1.53	8.03	28
1000	1.96	7.97	50
1500	2.95	7.87	60
2000	3.64	8.02	118
2500	4.61	8.13	190

is the Faraday constant (96485 C/mol), and A is the effective anode surface area (0.0075 m^2).

The ammonium removal efficiency (E_{rem}) was calculated with Eq. (2), where $NH_4^+\_N_{influent, anolyte}$ is the influent concentration (g/L), and $NH_4^+\_N_{effluent, anolyte}$ is the effluent concentration (g/L).

$$E_{rem}(\%) = \frac{NH_4^+\_N_{influent,anolyte} - NH_4^+\_N_{effluent,anolyte}}{NH_4^+\_N_{influent,anolyte}} \cdot 100 \quad (2)$$

The ammonium removal rate (R_{rem}) was calculated as ammonium removed from the anolyte and normalized by the CEM area with Eq. (3), where V_a is the anolyte volume treated (L), A_{CEM} is the CEM surface area (m^2), and t is time (d).

$$R_{rem} = \frac{\left(NH_4^+\_N_{influent,anolyte} - NH_4^+\_N_{effluent,anolyte}\right) \cdot V_a}{A_{CEM} \cdot t} \quad (3)$$

The ammonium recovery rate (R_{rec}) was calculated with Eq. (4), where $NH_4\_N_{final, recovery}$ and $NH_4\_N_{initial, recovery}$ are the final and initial concentrations in the recovery chamber (g/L), V_r is the recovery solution volume (L), and A_T is the Tyvek membrane surface area (m^2).

$$R_{rec} = \frac{\left(NH_4^+\_N_{final,recovery} - NH_4^+\_N_{initial,recovery}\right) \cdot V_r}{A_T \cdot t} \quad (4)$$

The ammonium recovery efficiency (E_{rec}) was calculated as a correlation between the final amount of ammonium in the recovery solution and the initial amount of ammonium in the anolyte (Eq. (5)).

$$E_{rec}(\%) = \frac{NH_4^+\_N_{final,recovery} \cdot V_r}{NH_4^+\_N_{initial,anolyte} \cdot V_a} \cdot 100 \quad (5)$$

The coulombic efficiency (CE) is the proportion between electron moles extracted as current intensity to the total electron moles made available from substrate oxidation (Eq. (6)).

$$CE(\%) = \frac{\int_{t_0}^{t_F} I \cdot dt}{V_L \cdot b_s \cdot F \cdot \Delta C \cdot M_s^{-1}} \cdot 100 \quad (6)$$

Where t_0 and t_F (s) are the times before and after renewing medium, I (A) is current, V_L (L) is the anolyte volume, b_s is the number of e$^-$ transferred per mole of acetate, ΔC (g/L) is the difference between initial and final acetate concentration, and M_s (g/mol) is the molecular weight of the acetate.

The energy consumption for the ammonium removal and recovery was calculated based on the removed ammonium and the electrical energy input of the MEC.

The total energy consumption of the system was calculated as Eqs. (7), (8) and (9):

$$W = W_{cell} + W_{pump} \quad (7)$$

$$W_{cell} = V \cdot I \quad (8)$$

$$W_{pump} = 3 \cdot Q \cdot \gamma \cdot E \cdot t / 1000 \quad (9)$$

Where W_{cell} (kWh) represents the electric input for the system while W_{pump} (kWh) is the electric consumption of the peristaltic pumps; V stands for the applied voltage (V), I is the measured intensity (A), and t denotes the operation time while Q is flow rate (m^3/s), γ is 9800 N/m^3, and E represents the hydraulic pressure head (m) [43].

3. Results and discussion

3.1. Current density

MECs anodes were run under continuous mode to assess how microorganisms adapted to high inlet ammonium concentrations. In Fig. 2, the current density achieved for different inlet ammonium concentrations and cathode materials is displayed. Current density represents the electric current passing through a unit cross-sectional area. Given a constant area, the current density illustrates the capacity of the biofilm to produce electrons, allowing the transfer of ammonium molecules from the anode chamber to the cathode chamber [44]. To preserve electroneutrality, one cation is transported from the anode chamber to the cathode chamber for every electron flowing through the external
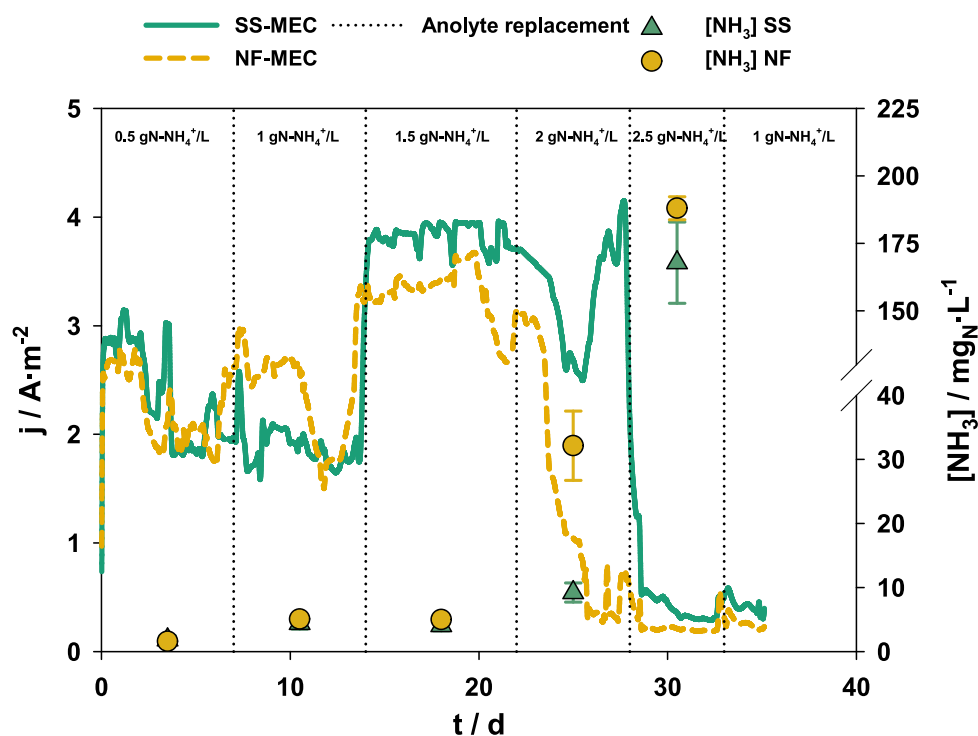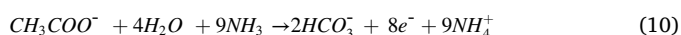

Fig. 2. Current density and free ammonia concentrations obtained for different influent NH_4^+ concentrations and cathode materials.

circuit [31]. Hence, anodic ammonium removal is directly linked to current density, indicating the highest migration rate possible.

Raising the influent ammonium concentration from 0.5 to 1 g N-NH$_4^+$/L resulted in a slight uptick in current density, as shown in Fig. 2. The maximum current density rose from 2.8 to 3.4 A/m^2 for NF-MEC and from 3.2 to 3.4 A/m^2 for SS-MEC. However, a subsequent increase of 1.5 g N-NH$_4^+$/L led to a plateau in current density. The highest achieved current density was 4.1 A/m^2 at 2 g N-NH$_4^+$/L for the SS cathode. This escalation in current density with higher influent ammonium concentrations can be attributed to enhanced anolyte conductivity, which reduces the ohmic overpotentials associated with ion migration. The medium conductivity ranged from 1.5 to 4.6 mS/cm (from lower to higher ammonium concentrations). Kim et al. [24] observed a rise in power density correlating with a rise in conductivity ranging from 8 mS/cm (84mg$_N$/L) to 14.4 mS/cm (1000 mg$_N$/L), attributed to higher ammonium concentration. However, continuous operation with ammonium eventually resulted in a power density plateau at 3.5g$_N$/L, mirroring the observations made in this study. The highest current density (4.1 A/m^2) was observed at 3.6 mS/cm. This result confirms that not only the ARB became resilient to the inhibitory stress caused by ammonium concentrations (up to 1.5 gN-NH$_4^+$/L) but also improved their performance.

Ledzema et al. [30] explained that microorganisms adapted to high ammonium concentration in a stepwise manner could become haloalkaliphilic and can use ammonia as a buffer, protonating it and reducing its adverse effects [26] as described in Eq. (10):

$$CH_3COO^- + 4H_2O + 9NH_3 \rightarrow 2HCO_3^- + 8e^- + 9NH_4^+ \quad (10)$$

Upon increasing ammonium concentration in the influent to 2 g N-NH$_4^+$/L with NF-MEC and to 2.5 g N-NH$_4^+$/L with SS-MEC, the current density significantly decreased to 0.5 A/m^2. Despite the enhanced resilience provided by continuous operation in systems dealing with higher ammonium concentrations, there exists a threshold concentration that triggers an inhibitory effect related to free ammonia. Fig. 2 shows how the free ammonia values increased at higher influent ammonium concentrations. In our study, the inhibitory threshold was identified in the range of ammonium influent concentrations of 2 g N-NH$_4^+$/L and 2.5 g N-NH$_4^+$/L. As can be observed, the value of free ammonia for NF-MEC was higher and it explains the higher inhibitory effect (i.e. lower current density) observed with this material.

In the realm of literature, there are two predominant theories addressing ammonia inhibition. The first theory proposes that unionized ammonia directly impairs cytosolic enzyme activity, while the second proposes that hydrophobic molecular ammonia, upon passive diffusion into the cell, rapidly converts to ammonium due to the intracellular pH [45]. The absence of an inhibition effect at lower ammonium concentrations in the anolyte could be ascribed to the solution having a pH below 7, leading to notably lower concentrations of free ammonia (up to 5 mgN/L) (Fig. 2). In contrast, a higher inlet ammonium concentration of 2500 mgN/L led to significantly elevated levels of free ammonia (168 mgN/L for SS and 188 mgN/L for NF), thereby causing inhibition. According to our results, values of free ammonia higher than 30 mgN/L were deleterious for the cell activity. With rising ammonium concentrations in the influent, the current density decreased in tandem with increased free ammonia concentration. In both scenarios, an increased ammonium concentration can hinder cellular activity. However, existing research lacks consensus on the specific threshold ammonium concentration that triggers inhibitory effects on ARB. Various factors, such as operational methods, influent pH, substrate concentration, and operating temperature have been identified as variables influencing the ammonium concentration threshold leading to inhibition of ARB [23]. Notably, real digested sewage sludge reject water typically contains an average of around 1 g N-NH$_4^+$/L [41], a concentration that would not induce inhibition in the context of this study at the usual pH values.

In the context of current-driven ammonium removal, load ratios were calculated based on the measured current generated by the anodic biofilm and the ammonium loading rate. Fig. 3 illustrates a clear downward trend between load ratio and the concentration of ammonium in the feed. Except for experiments featuring the lowest ammonium concentration (0.5 g N-NH$_4^+$/L), the load ratio remained below 1 across all concentrations. This aligns with findings from previous studies on BESs for ammonium recovery [38,46–48]. Consequently, the generated current proved inadequate to transport all ammonium across the membrane in experiments with higher ammonium concentrations. Both SS-MEC and NF-MEC results indicated that lower ammonium concentrations correlated with higher load ratios. However, to achieve greater ammonium recovery, increasing the L$_n$ above 1 becomes imperative. This can be achieved either by enhancing the current density or by reducing the ammonium loading in the feed.

The ammonium concentration examined in this study mirrors the typical values found in real reject water. Consequently, reducing its concentration would decrease the HRT, leading to an increase in the required reactor volume and a decrease in ammonium concentration in the product. A more feasible solution could involve achieving a higher volumetric current density. Considering that volumetric current density (A/m^3) results from a combination of microbial activity (A/m^2) and volumetric surface area (m^2/m^3), emphasis should be placed on fostering biofilm development and the use of anodes featuring larger surface areas and low overpotential. Increasing the surface area of the electrode is a more practical approach, leading to enhanced current density per volumetric area. Conversely, microbial activity, affecting current density, is contingent on the properties of the organic matter, favouring easily biodegradable substrates when aiming for higher intensities.

Higher current densities were associated with increased ammonium concentrations in the recovery solution, with the peak concentration stabilizing at 3.9 g N-NH$_4^+$/L. The lowest ammonium concentration tested yielded the highest load ratio, causing less ammonium to diffuse and migrate into the recovery solution. Consequently, this led to a reduced concentration in the final product of 1.1 g N-NH$_4^+$/L.

3.2. Removal and recovery of ammonium and acetate removal

In BES, ammonium removal hinges on the electric current generated, which carries ammonium through the CEM from the anode compartment to the cathode compartment. The highest efficiency in removing ammonium from the feed was 71%, achieved with a concentration of 0.5 g N-NH$_4^+$/L (Fig. 4A). This efficiency stands out, being comparable to and even surpassing those reported in existing literature
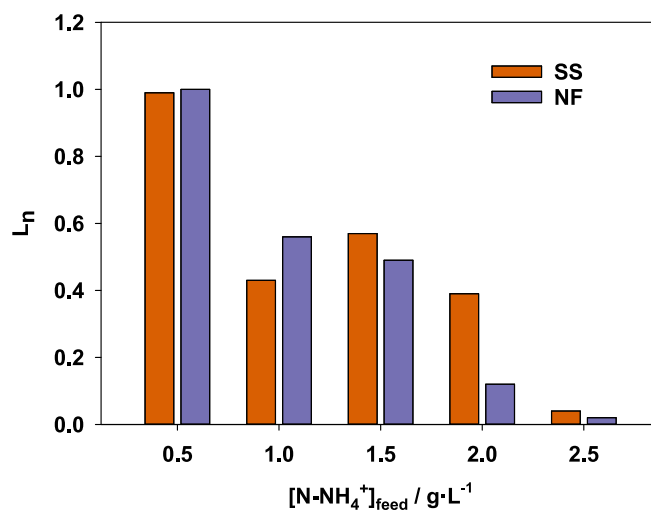

Fig. 3. Load ratio calculated for different ammonium concentrations in the feed.
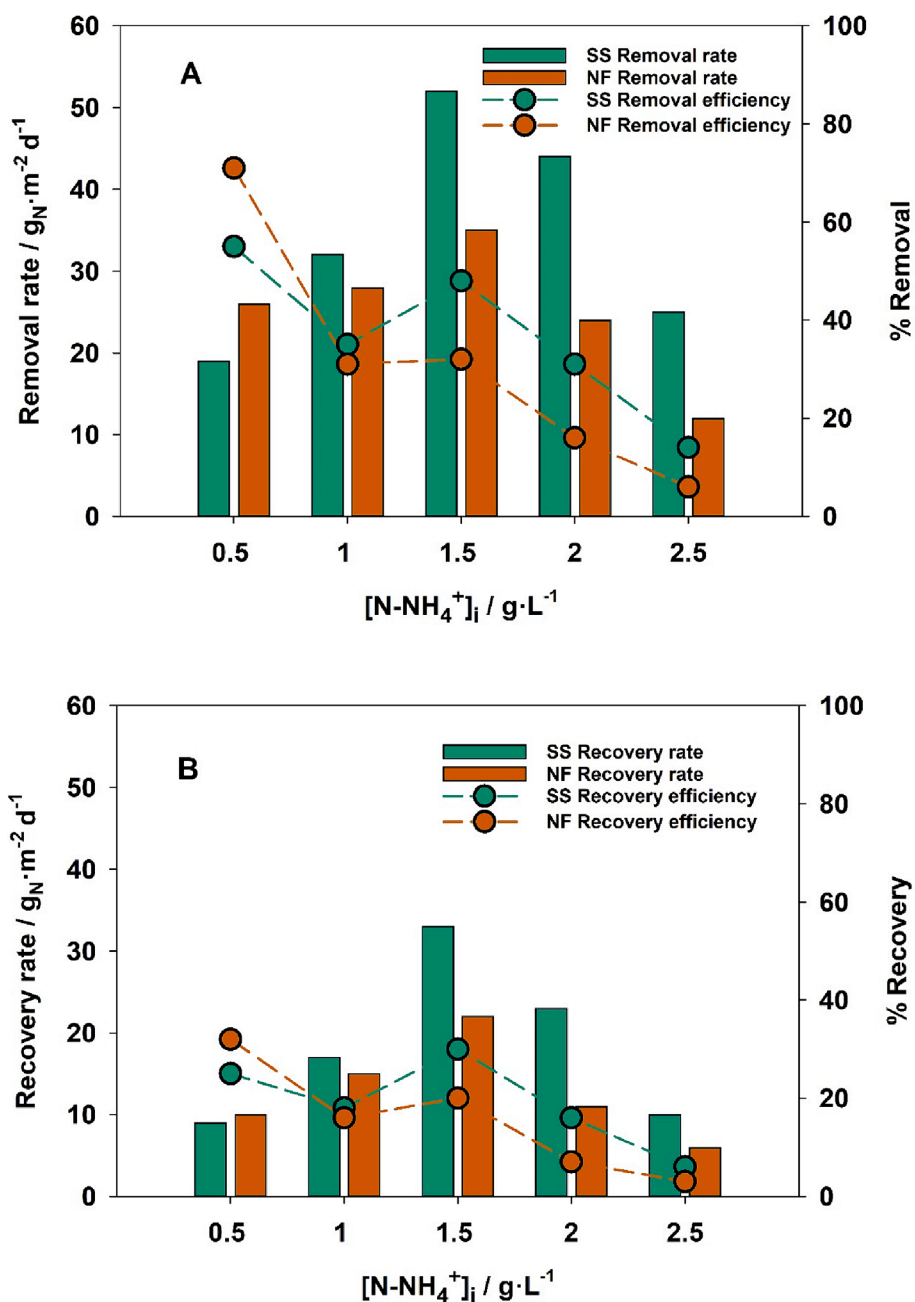
Fig. 4. Removal (A) and recovery (B) rates and efficiencies for different ammonium concentrations in the feed.

[31,37,38,46,48,49]. Notably, the load ratio for this ammonium concentration was nearly 1, theoretically indicating that the current density should be sufficient to eliminate all ammonium from the feed. However, the presence of other competing cations being transported across the CEM lowers the overall ammonium removal efficiency. Only 52.5% of electrons were attributed to the transfer of ammonium from the anolyte to the catholyte through the CEM when the concentration was 0.5 g N-NH_4^+/L.

Potassium and sodium ions were the main cations competing with ammonium for transport through the CEM due to their high concentrations in the anodic medium. This is evidenced by the fact that, in these experiments, 36% of the remaining electrons were allocated to the transport of sodium, while 5% were dedicated to potassium. This can be explained by the high permselectivity of membrane CMI-7000 for these three cations. It underscores the importance of considering their potential influence on diminishing the efficiency of ammonium removal.

Losantos et al. [34] also examined the migration of cations from the anolyte to assess the transport efficiency of the CEM and its implications for N-NH_4^+ removal. According to their findings, Na^+ contributed to nearly 50% of the positive charge balance, closely followed by NH_4^+ at almost 40%, with K^+ having very little impact. Kuntke et al. [25] also noted that ammonium and sodium played nearly equal roles in maintaining charge balance across the membrane, with potassium following behind.

As the ammonium concentration in the feed increased, the removal efficiency decreased, aligning with the declining load ratio observed at higher ammonium concentrations. The decline in removal efficiency is attributed to inadequate current, preventing the effective transport of higher concentrations of ammonium from the anolyte to the catholyte. Even if the entire intensity was dedicated to ammonium transport, it remains insufficient to transport all the ammonium. However, this trend confirms that a lower load ratio indicates lower ammonium removal

from the anodic compartment, as noted in previous research [32]. In general, the achieved ammonium removal efficiencies were notably high, 71% (NF-MEC) and 55% (SS-MEC) for 0.5 g N-NH$_4^+$/L and 48% (SS-MEC) and 32% (NF-MEC) for 1.5g N-NH$_4^+$/L, indicating effective utilization of the generated current for ammonium transport to the cathode. The SS-MEC demonstrated a maximum ammonium removal rate of 52 g$_N$/m^2/d, corresponding to an inlet ammonium concentration of 1.5 g N-NH$_4^+$/L.

In the second step of ammonium recovery, ammonia is extracted from the catholyte into the recovery solution using a gas-permeable hydrophobic membrane. The most efficient ammonium recovery (32%) was achieved with a feed concentration of 0.5 g N-NH$_4^+$/L (Fig. 4B). The driving force for ammonia transport through the gas-permeable membrane was the gradient in ammonia concentration between the catholyte and the recovery solution.

The relatively low recovery efficiency was likely due to the pH of the catholyte. Considering the pKa of the ammonia/ammonium equilibrium, at a pH of 9.25 roughly 50% of the ammonium exists as ammonia and the rest as ammonium. Since the experiments showed an average catholyte pH ranging from 8 to 9.5 the dominant form of ammonium/ammonia fluctuated, being the ammonia gradient limited during a significant fraction of the tests. As anticipated, a less alkaline pH led to high ammonium concentrations in the catholyte, suggesting a limitation in the transport rate of ammonia between the cathode and recovery chamber. Even for the ammonium concentration that led to the highest recovery efficiency (0.5 g N-NH$_4^+$/L), the ammonium concentration in the catholyte was higher (1.4 g N-NH$_4^+$/L) than the recovery solution (1.1 g N-NH$_4^+$/L). Apart from this, there is also the potential for ammonia loss as it may be stripped out of the chamber along with H$_2$, leading to reduced efficiency and recovery rates. Therefore, not all the removed ammonium from the anode was recovered as ammonium sulphate.

While this study employed batch mode for the recovery solution to achieve a concentrated stream of ammonium sulphate, a continuous flow of the recovery solution would improve removal and recovery outcomes by addressing mass transfer limitations and enabling lower ammonium concentrations in the recovery chamber. As the catholyte acts as an intermediate between the anolyte and the recovery solution, ideally, all ammonium from the anolyte should be converted to ammonia in the catholyte due to a high pH. A continuous feeding of the catholyte solution could lead to lower recovery efficiencies due to some ammonium ending up in the catholyte effluent, but recirculation of the catholyte solution could improve the mass transfer by assisting in maintaining the ammonium concentration low on the CEM-catholyte interface.

The highest flux from the cathode to the recovery chamber reached 33 gN/m^2/d. This recovery rate surpasses those reported in similar studies on ammonium recovery from digested sewage sludge reject waters [41,50] and aligns closely with the rate documented by Hou et al. (36 g$_N$/m^2/d) [35]. These findings highlight that the performance of the examined MEC is comparable to other systems utilized for ammonium recovery from reject water.

When the anolyte was fed with 2 g N-NH$_4^+$/L of ammonium, resulting in the highest achieved current density, the corresponding CE reached 86% with SS cathode. High CE (>60% in most cases) (Table 2) indicated that ARB efficiently oxidized acetate to generate electric current, thereby constraining methane production. This outcome mirrors

findings from a prior study utilizing a MEC to treat urine, where a gas-permeable membrane was employed to recover ammonia from the catholyte. In that study [46], a CE of 78% and a COD removal of 40% were reported, aligning with the results observed here.

Regarding other possible N-compounds, nitrite and nitrate were not detected in the anolyte effluent, as expected due to the lack of oxygen in the anode. Finally, acetate persisted in the anolyte effluent throughout all experiments, as the removal efficiency never exceeded 52%, and indicating that carbon source availability was not a limiting factor during the operation of the MECs.

3.3. Energy efficiencies

Electric energy calculations for both ammonium removal and recovery were conducted for all experiments. The total energy consumption was determined by considering the electric input from the applied voltage and anolyte pumping. The resulting estimated energy consumption is illustrated in Fig. 5.

Fig. 5A shows that the energy consumption for ammonium removal, considering both the energy from the applied voltage and pumping, was approximately 4 kWh/kg$_N$. These figures are notably lower than the energy consumption reported in the literature for BES with an integrated stripping method (Table 3). While the energy consumption for ammonia removal via stripping significantly fluctuates with operational conditions, it remained higher than that observed in the present study. Moreover, most previous studies did not account for the energy

Table 2
Coulombic efficiency obtained for different inlet ammonium concentrations.

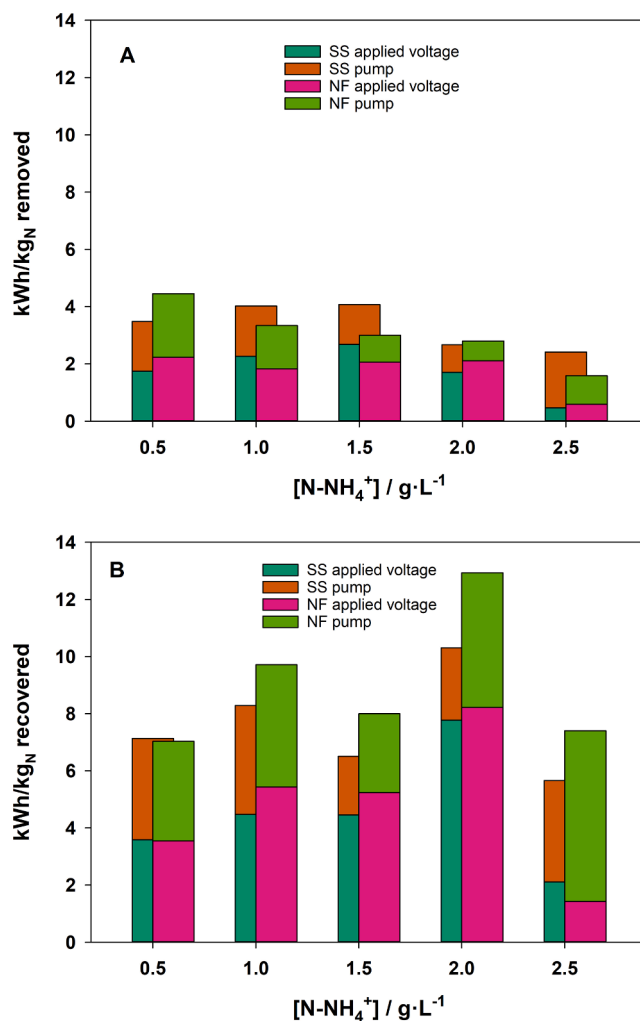| [Inlet NH$_4^+$] gN/L	CE (%) SS-MEC	CE (%) NF-MEC
0.5	76	57
1	73	77
1.5	75	76
2	86	63
2.5	55	35

Fig. 5. Energy consumption per kg$_N$ removed (A) and kg$_N$ recovered (B).

Table 3

Comparison among different studies concerning energy consumption of different recovery methods.

Wastewater	Recovery method	Inlet N-NH$_4^+$ concentration (g/L)	Cathode Material	Voltage (V)	Current density (A/m^2)	Energy consumption (kWh/kg$_N$)	Study
Synthetic reject water	TMCS	0.5	SS	1.4	2.2	*2.2 3.6	This study
		1.0			1.8	*1.8 4.5	
		1.5			3.8	*2.1 4.5	
		2.0			3.7	*2.1 7.8	
		2.5			0.4	*0.6 2.1	
Synthetic reject water	TMCS	0.5	NF	1.4	2.2	*1.8 3.5	This study
		1.0			1.9	*2.3 5.4	
		1.5			3.3	*2.7 5.2	
		2.0			2.2	*1.7 8.2	
		2.5			0.2	*0.5 1.4	
Synthetic digestate	Stripping	5.0	SS	3.3	11.3	*16.8 [a]	[37]
Digestate	Stripping	2.1	SS	3.5	7.5	*26.0 [a]	[37]
Synthetic medium	Stripping	5.0	SS	3.3	30.0	*16.8 [a]	[38]
Synthetic medium	Stripping	2.1	SS	2.1	27.0	*6.0 [a]	[38]
Synthetic blackwater	Stripping	1.0	GDE	0.2	2.5	*1.6 [a] *10.8 [b]	[34]
Effluent of MAP reactor	TMCS	3.4	Ti plate with MMO coating	0.8	1.7	0.4	[48]
Digestate	TMCS	1.5	SS	Poised anode (0V at Ag/AgCl)	3.6	5.0	[51]
Synthetic	TMCS	1.0	GDE	0.8	25.5	1.6	[35]
Synthetic	Stripping	1	Steel wire	Poised anode (0V at Ag/AgCl)	1.6	9.9 [a]	[39]
Synthetic	Stripping	0.8	Pt/C coated carbon cloth	0.8	1	4.5 [a]	[54]
Synthetic	Stripping	0.8	A/C coated carbon cloth	0.8	0.01 A [c]	1.3 [a]	[55]
Synthetic	Stripping	2.5	SS	Poised anode (-0.2V at Ag/AgCl)	9.4 [c]	3.6 [a]	[56]

TMCS = transmembrane chemisorption, A/C = activated carbon, GDE= gas diffusion electrode, MMO= mixed metal oxide *kg$_N$ removed

[a] without considering air stripping,

[b] considering air stripping,

[c] maximum value obtained

expended in the stripping process; they solely focused on electric energy input. An exception to this was the study by Losantos et al. [34], reporting an energy consumption of 10.8 kWh/kg$_N$ removed. The values obtained in our study for energy consumed/kg$_N$ removed are at least 50% lower than all the reported values.

On the contrary, reported electrical consumption per recovered ammonium in the literature shows a significant variation ranging from 3.8 to 40.9 kWh/kg$_N$ [37,39]. Most of these studies calculating electrical energy do not encompass the energy used for stripping and pumping. Nevertheless, the values obtained in this study fall at the lower end of the reported energy requirements and are competitive with the energy used in the Haber-Bosch process. While the specific energy consumption is low, it is achieved at the cost of the recovery rate. The highest achieved ammonium recovery rate was 33 g$_N$/m^2/d (for 1.5 gN-NH$_4^+$/L) with an associated energy consumption of 4.5 kWh/kg $_{N\ recovered}$. Conversely, a lower recovery rate of 10 g$_N$/m^2/d for 2.5 gN-NH$_4^+$/L resulted in a reduced energy consumption of 2.1 kWh/kg $_{N\ recovered}$. This highlights the inherent trade-off between energy consumption and the efficiency of ammonium recovery in the process.

Notably, only a few studies have mentioned energy consumption values for ammonium recovery in MECs employing hydrophobic membranes (without considering the energy used by pumps). The values obtained in this study closely align with the 5 kWh/kgN reported by Cerrillo et al. [51]. Hou et al. [35] managed to reduce the electrical energy consumption to 1.6 kWh/kg$_N$, similar to what was obtained in our study for influent ammonium concentrations of 2.5 g N-NH$_4^+$/L (2.1 kWh/kg$_N$ for SS; 1.4 kWh/kg$_N$ for NF). However, this concentration proved inhibitory in our study. Another study utilizing gas-permeable hydrophobic tubular membranes for ammonia recovery indicated an energy demand of 2.5 kWh/kg$_N$. Nevertheless, this lower energy demand was a result of the constantly replenished catholyte (leading to lower potential losses) and without considering energy used by pumps [46].

Our study analysis of pump-related energy consumption emphasizes its noteworthy influence on the overall energy demands, a factor often omitted in other research studies. However, Ward et al. [52] clarified that the additional energy consumption attributed to pumping could be considerably high on a laboratory scale (~5 kWh/kg$_N$), primarily due to peristaltic pumps. Yet, due to the relatively low pressure drop on the diluent side, the energy needed for pumping would be notably lower on a larger scale, approximately on the order of 0.1 kWh/m^3 compared to the electrochemical energy requirement.

In summary, the energy consumption observed in this study, using synthetic reject water, aligns comparably with other BESs. Additionally, these values are lower than the combined energy requirement (25 kWh/kg$_N$) reported for nitrogen removal in activated sludge processes and nitrogen fixation through the Haber-Bosch method [53]. This indicates the promising potential of the studied technology for efficient ammonium recovery.

To further minimize energy demands, emphasis should be placed on reducing electrochemical losses, particularly cell voltage, through optimization of electrode materials and minimizing the distance between electrodes. Enhancing membranes would also lead to further efficiency gains. Additionally, potential benefits from the produced hydrogen should be taken into account for ammonium recovery. The recovered hydrogen energy content has the potential to significantly decrease energy demands, or utilizing hydrogen for on-site energy needs can open economic opportunities for WWTPs and anaerobic digestion facilities, potentially offsetting some operational expenses.

3.4. Electrochemical measurements

Before increasing the inlet ammonium concentration, the chronoamperometry experiments were paused to record CV curves. Fig. 6 displays the CVs recorded at the anode for SS-MEC and NF-MEC at a scan rate of 5 mV/s. CV has been utilized as a non-intrusive method to investigate electroactive biofilms [57,58]. To mitigate the impact of any biological variability, varying ammonium concentrations were subsequently tested in the same reactor by changing the medium between experiments.

A significant contrast in electrochemical kinetics was evident at the highest ammonium concentrations tested (2.5 g N-NH$_4^+$/L) in both SS-MEC and NF-MEC. In terms of electrochemical kinetics, SS demonstrated superior performance by delivering slightly higher intensities at lower potentials. This preference for SS became more pronounced at higher potential values. CV analyses revealed that SS-MECs could reach a maximum intensity of up to 0.09 A at 1 V vs. Ag/AgCl (with 2 gN-NH$_4^+$/L), while NF-MEC never surpassed 0.05 A. The differences in most voltammetry curves were not substantial enough to reasonably infer that the 3D structure of NF might have a favourable effect.

In the SS-MEC, a clear correlation was observed between ammonium concentration and the oxidation potential of the active site: 0.71 V for 2 g N-NH$_4^+$/L, 0.76 V for 1.5 g N-NH$_4^+$/L, 0.83 V for 1g N-NH$_4^+$/L, and 0.88 V for 0.5g N-NH$_4^+$/L. Decreasing ammonium concentration led to a shift in the oxidation potential towards more positive values, indicating that extracellular electron transfer in the biofilm occurred at lower electrode potentials, generating higher intensity. However, when the biofilm was exposed to 2.5 g N-NH$_4^+$/L, no consistent and distinctive CV curve was observed, suggesting possible biofilm inhibition. The change in CV profile for 2.5 g N-NH$_4^+$/L of ammonium in the feed might be due to an increase in inactive biofilm affecting electrochemical reactions.

In the NF-MEC, the catalytic current showed minimal change upon increasing the ammonium concentration up to 1.5 g N-NH$_4^+$/L in the anolyte. The maximum current remained very close (0.36 A for 0.5-1 g N-NH$_4^+$/L and 0.044 A for 1.5-2 g N-NH$_4^+$/L at 1 V), indicating little difference in ARB activity under these conditions. Another study demonstrated similar CV curve intensities (0.03 A) for an inlet ammonium concentration of 0.9 g N-NH$_4^+$/L, but observed a significant decrease (0.009 A) at a slightly higher concentration of 1.2 g N-NH$_4^+$/L [45]. The catalytic current notably dropped at an ammonium concentration of 2 g N-NH$_4^+$/L, indicating weakened electrocatalytic activity. Likewise, a distinctly different CV curve was observed at 2.5 g N-NH$_4^+$/L, suggesting that ammonium concentrations could substantially impact ARB activity.

4. Conclusions

The experimental findings indicated the feasibility of applying high influent ammonium concentrations in a continuously fed MEC provided the removal is high and the pH is low enough to maintain a low free ammonia concentration. The recommended threshold for maximum ammonium in wastewater is suggested to be approximately 20-30 mg NH$_3$/L. Higher concentrations induced a reduction in current generation, as evidenced by cyclic voltammograms.

The primary cation transferred from the anolyte to the catholyte was ammonium, accounting for 53% of electrons attributed to its transfer through the CEM.

Two distinct cathode materials (SS and NF) were employed in these assessments. Notably, higher current densities achieved with SS resulted in higher removal and recovery rates, along with increased efficiencies. The higher current density facilitated the extraction of ammonium ions from the anolyte, leading to a decreased concentration of free ammonia, a known toxic factor for ARB. The highest ammonium removal efficiency was 71% obtained with 0.5 g N-NH$_4^+$/L.

Moreover, energy consumption was also assessed per kilogram of nitrogen removed and recovered for all the tested conditions. The maximum ammonium recovery rate achieved was 33 g$_N$/m^2/d (for 1.5 gN-NH$_4^+$/L) with an associated energy consumption of 4.5 kWh/kgN recovered. In contrast, a lower recovery rate of 10 g$_N$/m^2/d for 2.5 gN-NH$_4^+$/L led to a decreased energy consumption of 2.1 kWh/kgN recovered. This underscores the intrinsic trade-off between energy consumption and effective ammonium recovery in the process.

In this study, the current density emerged as a constraining factor for ammonium removal from the anolyte, as evidenced by the load ratio values. Except for experiments involving the lowest ammonium concentration (0.5 g N-NH$_4^+$/L), the load ratio stayed below 1 for all other concentrations indicating that current density was not high enough to transport all the ammonium from the anolyte to the catholyte. Concerning ammonium recovery, the catholyte pH was identified as the restricting factor for converting ammonium to ammonia. Consequently, maintaining a pH above 9.25 is deemed necessary to facilitate the improved recovery of ammonia through the hydrophobic membrane.

CRediT authorship contribution statement

Zainab Ul: Writing – original draft, Visualization, Methodology, Investigation, Formal analysis, Data curation, Conceptualization. **Mira Sulonen:** Writing – review & editing, Supervision, Methodology, Investigation, Formal analysis. **Juan Antonio Baeza:** Writing – review & editing, Visualization, Validation, Supervision, Software,
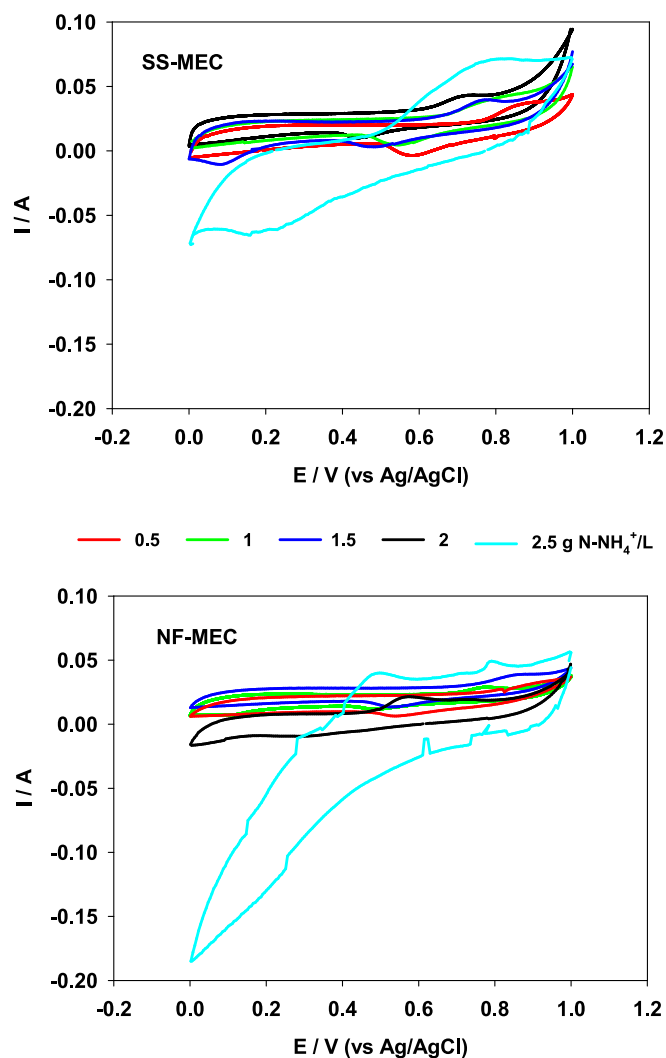

Fig. 6. Anodic cyclic voltammograms observed for different ammonium concentrations in the feed.

Methodology, Investigation, Formal analysis, Conceptualization. **Albert Guisasola:** Writing – review & editing, Validation, Supervision, Resources, Project administration, Methodology, Funding acquisition, Formal analysis, Conceptualization.

Declaration of competing interest

The authors declare that they have no known competing financial interests or personal relationships that could have appeared to influence the work reported in this paper.

Data availability

Data will be made available on request.

Acknowledgements

References

[1] M. Rodríguez Arredondo, P. Kuntke, A.W. Jeremiasse, T.H.J.A. Sleutels, C.J. N. Buisman, A. ter Heijne, Bioelectrochemical systems for nitrogen removal and recovery from wastewater, Environ. Sci.: Water Res. Technol. 1 (2015) 22–33, https://doi.org/10.1039/C4EW00066H.

[2] D. Hou, L. Lu, Z.J. Ren, Microbial fuel cells and osmotic membrane bioreactors have mutual benefits for wastewater treatment and energy production, Water Res. 98 (2016) 183–189, https://doi.org/10.1016/j.watres.2016.04.017.

[3] T.C. Jorgensen, L.R. Weatherley, Ammonia removal from wastewater by ion exchange in the presence of organic contaminants, Water Res. 37 (2003) 1723–1728, https://doi.org/10.1016/S0043-1354(02)00571-7.

[4] W. Pronk, M. Biebow, M. Boller, Electrodialysis for Recovering Salts from a Urine Solution Containing Micropollutants, Environ. Sci. Technol. 40 (2006) 2414–2420, https://doi.org/10.1021/es051921i.

[5] K.M. Udert, M. Wächter, Complete nutrient recovery from source-separated urine by nitrification and distillation, Water Res. 46 (2012) 453–464, https://doi.org/10.1016/j.watres.2011.11.020.

[6] Y.V. Nancharaiah, S. Venkata Mohan, P.N.l. Lens, Recent advances in nutrient removal and recovery in biological and bioelectrochemical systems, Bioresour. Technol. 215 (2016) 173–185, https://doi.org/10.1016/j.biortech.2016.03.129.

[7] P. Kuntke, T.H.J.A. Sleutels, M. Rodríguez Arredondo, S. Georg, S.G. Barbosa, A. Ter Heijne, H.V.M. Hamelers, C.J.N. Buisman, (Bio)electrochemical ammonia recovery: progress and perspectives, Appl Microbiol Biotechnol 102 (2018) 3865–3878, https://doi.org/10.1007/s00253-018-8888-6.

[8] Y.-J. Lee, B.-L. Lin, M. Xue, K. Tsunemi, Ammonia/ammonium removal/recovery from wastewaters using bioelectrochemical systems (BES): A review, Bioresour. Technol. 363 (2022) 127927, https://doi.org/10.1016/j.biortech.2022.127927.

[9] T.-J.-P. Ivase, B.B. Nyakuma, O. Oladokun, P.T. Abu, M.N. Hassan, Review of the principal mechanisms, prospects, and challenges of bioelectrochemical systems, Environ Prog Sustainable Energy 39 (2020) 13298, https://doi.org/10.1002/ep.13298.

[10] K.Y. Cheng, A.H. Kaksonen, R. Cord-Ruwisch, Ammonia recycling enables sustainable operation of bioelectrochemical systems, Bioresour. Technol. 143 (2013) 25–31, https://doi.org/10.1016/j.biortech.2013.05.108.

[11] R.A. Rozendal, H.V.M. Hamelers, C.J.N. Buisman, Effects of membrane cation transport on pH and microbial fuel cell performance, Environ. Sci. Technol. 40 (2006) 5206–5211, https://doi.org/10.1021/es060387r.

[12] X.-T. Wang, Y.-F. Zhang, B. Wang, S. Wang, X. Xing, X.-J. Xu, W.-Z. Liu, N.-Q. Ren, D.-J. Lee, C. Chen, Enhancement of methane production from waste activated sludge using hybrid microbial electrolysis cells-anaerobic digestion (MEC-AD) process – A review, Bioresour. Technol. 346 (2022) 126641, https://doi.org/10.1016/j.biortech.2021.126641.

[13] Z. Zhang, Z. Wang, J. Zhang, R. Deng, H. Peng, Y. Guo, P. Xiang, S. Xia, Ammonia recovery from wastewater using a bioelectrochemical membrane-absorbed ammonia system with authigenic acid and base, J. Clean. Prod. 296 (2021) 126554, https://doi.org/10.1016/j.jclepro.2021.126554.

[14] I. Angelidaki, B.K. Ahring, Thermophilic anaerobic digestion of livestock waste: the effect of ammonia, Appl Microbiol Biotechnol 38 (1993), https://doi.org/10.1007/BF00242955.

[15] A.K. Luther, Ammonia toxicity in bacteria and its implications for treatment of and resource recovery from highly nitrogenous organic wastes. https://doi.org/10.7282/T3668G53.

[16] T. Müller, B. Walter, A. Wirtz, A. Burkovski, Ammonium toxicity in bacteria, Curr Microbiol 52 (2006) 400–406, https://doi.org/10.1007/s00284-005-0370-x.

[17] M.L. Garcia, L.T. Angenent, Interaction between temperature and ammonia in mesophilic digesters for animal waste treatment, Water Res. 43 (2009) 2373–2382, https://doi.org/10.1016/j.watres.2009.02.036.

[18] K.H. Hansen, I. Angelidaki, B.K. Ahring, Anaerobic digestion of swine manure: inhibition by ammonia, Water Res. 32 (1998) 5–12, https://doi.org/10.1016/S0043-1354(97)00201-7.

[19] J.-Y. Nam, H.-W. Kim, H.-S. Shin, Ammonia inhibition of electricity generation in single-chambered microbial fuel cells, J. Power Sources 195 (2010) 6428–6433, https://doi.org/10.1016/j.jpowsour.2010.03.091.

[20] S. Poirier, E. Desmond-Le Quéméner, C. Madigou, T. Bouchez, O. Chapleur, Anaerobic digestion of biowaste under extreme ammonia concentration: Identification of key microbial phylotypes, Bioresour. Technol. 207 (2016) 92–101, https://doi.org/10.1016/j.biortech.2016.01.124.

[21] J. Procházka, P. Dolejš, J. Máca, M. Dohányos, Stability and inhibition of anaerobic processes caused by insufficiency or excess of ammonia nitrogen, Appl Microbiol Biotechnol 93 (2012) 439–447, https://doi.org/10.1007/s00253-011-3625-4.

[22] M. Mahmoud, P. Parameswaran, C.I. Torres, B.E. Rittmann, Electrochemical techniques reveal that total ammonium stress increases electron flow to anode respiration in mixed-species bacterial anode biofilms: Ammonia Stress Increases Respiration Rate of Anode Biofilms, Biotechnol. Bioeng. 114 (2017) 1151–1159, https://doi.org/10.1002/bit.26246.

[23] R.C. Tice, Y. Kim, Influence of substrate concentration and feed frequency on ammonia inhibition in microbial fuel cells, J. Power Sources 271 (2014) 360–365, https://doi.org/10.1016/j.jpowsour.2014.08.016.

[24] H.-W. Kim, J.-Y. Nam, H.-S. Shin, Ammonia inhibition and microbial adaptation in continuous single-chamber microbial fuel cells, J. Power Sources 196 (2011) 6210–6213, https://doi.org/10.1016/j.jpowsour.2011.03.061.

[25] P. Kuntke, M. Geleji, H. Bruning, G. Zeeman, H.V.M. Hamelers, C.J.N. Buisman, Effects of ammonium concentration and charge exchange on ammonium recovery from high strength wastewater using a microbial fuel cell, Bioresour. Technol. 102 (2011) 4376–4382, https://doi.org/10.1016/j.biortech.2010.12.085.

[26] P. Kuntke, K.M. Śmiech, H. Bruning, G. Zeeman, M. Saakes, T.H.J.A. Sleutels, H.V. M. Hamelers, C.J.N. Buisman, Ammonium recovery and energy production from urine by a microbial fuel cell, Water Res. 46 (2012) 2627–2636, https://doi.org/10.1016/j.watres.2012.02.025.

[27] H. Lin, X. Wu, C. Nelson, C. Miller, J. Zhu, Electricity generation and nutrients removal from high-strength liquid manure by air-cathode microbial fuel cells, J. Environ. Sci. Health A 51 (2016) 240–250, https://doi.org/10.1080/10934529.2015.1094342.

[28] L. Wang, B. Xie, N. Gao, B. Min, H. Liu, Urea removal coupled with enhanced electricity generation in single-chambered microbial fuel cells, Environ. Sci. Pollut. Res. 24 (2017) 20401–20408, https://doi.org/10.1007/s11356-017-9689-7.

[29] P. Clauwaert, R. Tolêdo, D. Van Der Ha, R. Crab, W. Verstraete, H. Hu, K.M. Udert, K. Rabaey, Combining biocatalyzed electrolysis with anaerobic digestion, Water Sci. Technol. 57 (2008) 575–579, https://doi.org/10.2166/wst.2008.084.

[30] P. Ledezma, J. Jermakka, J. Keller, S. Freguia, Recovering nitrogen as a solid without chemical dosing: bio-electroconcentration for recovery of nutrients from urine, Environ. Sci. Technol. Lett. 4 (2017) 119–124, https://doi.org/10.1021/acs.estlett.7b00024.

[31] Y. Liu, M. Qin, S. Luo, Z. He, R. Qiao, Understanding ammonium transport in bioelectrochemical systems towards its recovery, Sci. Rep. 6 (2016) 22547, https://doi.org/10.1038/srep22547.

[32] M. Rodríguez Arredondo, P. Kuntke, A. ter Heijne, H.V.M. Hamelers, C.J. N. Buisman, Load ratio determines the ammonia recovery and energy input of an electrochemical system, Water Res. 111 (2017) 330–337, https://doi.org/10.1016/j.watres.2016.12.051.

[33] S. Haddadi, G. Nabi-Bidhendi, N. Mehrdadi, Nitrogen removal from wastewater through microbial electrolysis cells and cation exchange membrane, J. Environ. Health Sci. Engineer. 12 (2014) 48, https://doi.org/10.1186/2052-336X-12-48.

[34] D. Losantos, M. Aliaguilla, D. Molognoni, M. González, P. Bosch-Jimenez, S. Sanchis, A. Guisasola, E. Borràs, Development and optimization of a bioelectrochemical system for ammonium recovery from wastewater as fertilizer, Cleaner Engineering and Technology 4 (2021) 100142, https://doi.org/10.1016/j.clet.2021.100142.

[35] D. Hou, A. Iddya, X. Chen, M. Wang, W. Zhang, Y. Ding, D. Jassby, Z.J. Ren, Nickel-Based Membrane Electrodes Enable High-Rate Electrochemical Ammonia Recovery, Environ. Sci. Technol. 52 (2018) 8930–8938, https://doi.org/10.1021/acs.est.8b01349.

[36] M. Cerrillo, L. Burgos, E. Serrano-Finetti, V. Riau, J. Noguerol, A. Bonmatí, Hydrophobic membranes for ammonia recovery from digestates in microbial electrolysis cells: Assessment of different configurations, J. Environ. Chem. Eng. 9 (2021) 105289, https://doi.org/10.1016/j.jece.2021.105289.

[37] J. Desloover, A. Abate Woldeyohannis, W. Verstraete, N. Boon, K. Rabaey, Electrochemical resource recovery from digestate to prevent ammonia toxicity during anaerobic digestion, Environ. Sci. Technol. 46 (2012) 12209–12216, https://doi.org/10.1021/es3028154.

[38] S. Gildemyn, A.K. Luther, S.J. Andersen, J. Desloover, K. Rabaey, Electrochemically and bioelectrochemically induced ammonium recovery, JoVE (2015) 52405, https://doi.org/10.3791/52405.

[39] X. Wu, O. Modin, Ammonium recovery from reject water combined with hydrogen production in a bioelectrochemical reactor, Bioresour. Technol. 146 (2013) 530–536, https://doi.org/10.1016/j.biortech.2013.07.130.

[40] E. Arnold, B. Böhm, P.A. Wilderer, Application of activated sludge and biofilm sequencing batch reactor technology to treat reject water from sludge dewatering

systems: a comparison, Water Sci. Technol. 41 (2000) 115–122, https://doi.org/10.2166/wst.2000.0019.

[41] V. Koskue, J.M. Rinta-Kanto, S. Freguia, P. Ledezma, M. Kokko, Optimising nitrogen recovery from reject water in a 3-chamber bioelectroconcentration cell, Sep. Purif. Technol. 264 (2021) 118428, https://doi.org/10.1016/j.seppur.2021.118428.

[42] Z. Ul, P. Sánchez-Peña, M. Baeza, M. Sulonen, D. Gabriel, J.A. Baeza, A. Guisasola, Systematic screening of carbon-based anode materials for bioelectrochemical systems, J. of Chemical Tech & Biotech 98 (2023) 1402–1415, https://doi.org/10.1002/jctb.7357.

[43] Y. Zhang, I. Angelidaki, Recovery of ammonia and sulfate from waste streams and bioenergy production via bipolar bioelectrodialysis, Water Res. 85 (2015) 177–184, https://doi.org/10.1016/j.watres.2015.08.032.

[44] B.R. Dhar, H.-S. Lee, Evaluation of limiting factors for current density in microbial electrochemical cells (MXCs) treating domestic wastewater, Biotechnol. Rep. 4 (2014) 80–85, https://doi.org/10.1016/j.btre.2014.09.005.

[45] H. Wang, Y. Zhang, G. Wang, Ammonia Inhibition Effects on Performance of a Continuous Stirred Bioelectrochemical System, in: X. Zhang, H. Ren, Y. Lu, C. Wang (Eds.), Advances in Transdisciplinary Engineering, IOS Press, 2022, https://doi.org/10.3233/ATDE220345.

[46] P. Kuntke, P. Zamora, M. Saakes, C.J.N. Buisman, H.V.M. Hamelers, Gas-permeable hydrophobic tubular membranes for ammonia recovery in bio-electrochemical systems, Environ. Sci.: Water Res. Technol. 2 (2016) 261–265, https://doi.org/10.1039/C5EW00299K.

[47] M. Rodríguez Arredondo, P. Kuntke, A. Ter Heijne, C.J. Buisman, The concept of load ratio applied to bioelectrochemical systems for ammonia recovery, J. Chem. Technol. Biotechnol. 94 (2019) 2055–2061, https://doi.org/10.1002/jctb.5992.

[48] P. Zamora, T. Georgieva, A. Ter Heijne, T.H.J.A. Sleutels, A.W. Jeremiasse, M. Saakes, C.J.N. Buisman, P. Kuntke, Ammonia recovery from urine in a scaled-up Microbial Electrolysis Cell, J. Power Sources 356 (2017) 491–499, https://doi.org/10.1016/j.jpowsour.2017.02.089.

[49] P. Kuntke, T.H.J.A. Sleutels, M. Saakes, C.J.N. Buisman, Hydrogen production and ammonium recovery from urine by a Microbial Electrolysis Cell, Int. J. Hydrogen Energy 39 (2014) 4771–4778, https://doi.org/10.1016/j.ijhydene.2013.10.089.

[50] S. Barua, B.S. Zakaria, T. Chung, F.I. Hai, T. Haile, A. Al-Mamun, B.R. Dhar, Microbial electrolysis followed by chemical precipitation for effective nutrients recovery from digested sludge centrate in WWTPs, Chem. Eng. J. 361 (2019) 256–265, https://doi.org/10.1016/j.cej.2018.12.067.

[51] M. Cerrillo, L. Burgos, A. Bonmatí, Biogas upgrading and ammonia recovery from livestock manure digestates in a combined electromethanogenic biocathode—hydrophobic membrane system, Energies 14 (2021) 503, https://doi.org/10.3390/en14020503.

[52] A.J. Ward, K. Arola, E. Thompson Brewster, C.M. Mehta, D.J. Batstone, Nutrient recovery from wastewater through pilot scale electrodialysis, Water Res. 135 (2018) 57–65, https://doi.org/10.1016/j.watres.2018.02.021.

[53] M. Maurer, P. Schwegler, T.A. Larsen, Nutrients in urine: energetic aspects of removal and recovery, Water Sci. Technol. 48 (2003) 37–46, https://doi.org/10.2166/wst.2003.0011.

[54] M. Qin, Y. Liu, S. Luo, R. Qiao, Z. He, Integrated experimental and modeling evaluation of energy consumption for ammonia recovery in bioelectrochemical systems, Chem. Eng. J. 327 (2017) 924–931, https://doi.org/10.1016/j.cej.2017.06.182.

[55] M. Qin, C. White, S. Zou, Z. He, Passive separation of recovered ammonia from catholyte for reduced energy consumption in microbial electrolysis cells, Chem. Eng. J. 334 (2018) 2303–2307, https://doi.org/10.1016/j.cej.2017.11.190.

[56] A. Carucci, G. Erby, G. Puggioni, D. Spiga, F. Frugoni, S. Milia, Ammonium recovery from agro-industrial digestate using bioelectrochemical systems, Water Sci. Technol. 85 (2022) 2432–2441, https://doi.org/10.2166/wst.2022.113.

[57] E. Marsili, J.B. Rollefson, D.B. Baron, R.M. Hozalski, D.R. Bond, Microbial Biofilm Voltammetry: Direct Electrochemical Characterization of Catalytic Electrode-Attached Biofilms, Appl Environ Microbiol 74 (2008) 7329–7337, https://doi.org/10.1128/AEM.00177-08.

[58] D. Pocaznoi, A. Calmet, L. Etcheverry, B. Erable, A. Bergel, Stainless steel is a promising electrode material for anodes of microbial fuel cells, Energy Environ. Sci. 5 (2012) 9645, https://doi.org/10.1039/c2ee22429a.